NeuroImage: Clinical 19 (2018) 824–830

Contents lists available at ScienceDirect

NeuroImage: Clinical

journal homepage: www.elsevier.com/locate/ynicl

Comparison between simultaneously acquired arterial spin labeling and ^{18}F-FDG PET in mesial temporal lobe epilepsy assisted by a PET/MR system and SEEG

Yi-He Wang[a,1], Yang An[a,1], Xiao-Tong Fan[a], Jie Lu[b,c], Lian-Kun Ren[d], Peng-Hu Wei[a], Bi-Xiao Cui[c], Jia-Lin Du[d], Chao Lu[a], Di Wang[d], Hua-Qiang Zhang[a], Yong-Zhi Shan[a,*], Guo-Guang Zhao[a,e,*]

[a] Department of Neurosurgery, Xuanwu Hospital, Capital Medical University, Beijing 100053, China
[b] Department of Radiology, Xuanwu Hospital, Capital Medical University, Beijing 100053, China
[c] Department of Nuclear Medicine, Xuanwu Hospital, Capital Medical University, Beijing 100053, China
[d] Department of Neurology, Xuanwu Hospital, Capital Medical University, Beijing 100053, China
[e] Center of Epilepsy, Beijing Institute for Brain Disorder, Beijing 100069, China

ARTICLE INFO

Keywords:
Arterial spin labeling (ASL)
^{18}F-FDG PET
PET/MR
SEEG
Epilepsy

ABSTRACT

Objective: In the detection of seizure onset zones, arterial spin labeling (ASL) can overcome the limitations of positron emission tomography (PET) with ^{18}F-fluorodeoxyglucose (^{18}F-FDG), which is invasive, expensive, and radioactive. PET/magnetic resonance (MR) systems have been introduced that allow simultaneous performance of ASL and PET, but comparisons of these techniques with stereoelectroencephalography (SEEG) and comparisons among the treatment outcomes of these techniques are still lacking. Here, we investigate the effectiveness of ASL compared with that of SEEG and their outcomes in localizing mesial temporal lobe epilepsy (MTLE) and assess the correlation between simultaneously acquired PET and ASL.

Methods: Between October 2016 and August 2017, we retrospectively studied 12 patients diagnosed with pure unilateral MTLE. We extracted and quantitatively computed values for ASL and PET in the bilateral hippocampus. SEEG findings and outcome were considered the gold standard of lateralization. Finally, the bilateral asymmetry index (AI) was calculated to assess the correlation between PET and ASL.

Results: Our results showed that hypoperfusion in the hippocampus detected using ASL matched the SEEG-defined epileptogenic zone in this series of patients. The mean normalized voxel value of ASL in the contralateral hippocampus was 0.97 ± 0.19, while in the ipsilateral hippocampus, it was 0.84 ± 0.14. Meanwhile, significantly decreased perfusion and metabolism were observed in these patients (Wilcoxon, $p < 0.05$), with a significant positive correlation between the AI values derived from PET and ASL (Pearson's correlation, $r = 0.74$, $p < 0.05$).

Significance: In our SEEG- and outcome-defined patients with MTLE, ASL could provide significant information during presurgical evaluation, with the hypoperfusion detected with ASL reliably lateralizing MTLE. This non-invasive technique may be used as an alternative diagnostic tool for MTLE lateralization.

1. Introduction

During presurgical evaluation of mesial temporal lobe epilepsy (MTLE), a significant relationship between treatment outcome and accuracy in identifying the epileptogenic zone has been recognized (Hardy et al., 2003). Conventional non-invasive presurgical evaluation includes semiology, electroencephalography (EEG), structural imaging, and functional imaging (Chavakula and Cosgrove, 2017; Duncan, 2010; Fisher et al., 1997; Rosenow and Luders, 2001). In recent years, ^{18}F-fluorodeoxyglucose positron emission tomography (^{18}F-FDG PET) has been considered as the leading functional imaging option for presurgical evaluation during the interictal phase, particularly in patients with structural imaging-negative refractory epilepsy. This is because high consistency has been observed between regional hypometabolism and the epileptogenic zone (Rathore et al., 2014). However, there remain some limitations in the use of ^{18}F-FDG PET in clinical practice: 1) it is invasive and expensive, 2) it involves exposure to radiation, 3) it is unavailable in many epilepsy centers.

* Corresponding authors at: Department of Neurosurgery, Xuan Wu Hospital, Capital Medical University, No. 45, Changchun Street, Xuanwu District, Beijing 100053, China.
E-mail addresses: shanyongzhi@xwhosp.org (Y.-Z. Shan), ggzhao@vip.sina.com (G.-G. Zhao).
[1] Yi-He Wang and Yang An contributed equally to the study.

https://doi.org/10.1016/j.nicl.2018.06.008
Received 19 December 2017; Received in revised form 2 June 2018; Accepted 4 June 2018
Available online 07 June 2018

Notably, arterial spin labeling (ASL), a magnetic resonance (MR) imaging technique that measures perfusion, has been increasingly used to evaluate brain function in multiple neurological disorders in recent years (Blauwblomme et al., 2014; Boscolo Galazzo et al., 2015). It provides information on regional cerebral blood flow (CBF) by using magnetically-labeled arterial blood water as an endogenous contrast agent (Detre et al., 1992; Williams et al., 1992).

Previous studies have compared ^{18}F-FDG PET and ASL (Boscolo Galazzo et al., 2016; Kim et al., 2016; Storti et al., 2014; Wolf et al., 2001); however, many of them have failed to conduct further investigations involving simultaneous comparisons of the two modalities. PET and MRI co-registration images may exhibit limitations with respect to detection of seizure foci, since the two images are acquired at different times using different machines (Ding et al., 2014). Misregistration or various motion artifacts may introduce errors (Rakheja et al., 2013). A combined PET/MR scanner with simultaneous acquisition permits simultaneous imaging of physiological and pathophysiological processes and provides both anatomical and functional information on the same subject (Ding et al., 2014; Fraioli and Punwani, 2014; Tudisca et al., 2015). Thus, a better comparison of different modalities under identical conditions can be achieved with this system. One previous report has compared simultaneous ^{18}F-FDG PET and ASL with a PET/MR system, but it lacked a gold standard diagnosis for most of the included cases, with no invasive treatment and with unavailable outcome data (Boscolo Galazzo et al., 2016). To the best of our knowledge, few studies have investigated the correlations between PET and ASL, simultaneously acquired with PET/MR, and no previous study has systematically compared these with invasive techniques (stereo-electroencephalography, SEEG) and outcome in MTLE. Based on previous studies, we have conducted further investigations using SEEG and treatment outcome as gold standards to assess the usefulness of ASL, with data collected using combined PET-MRI, in patients with MTLE.

Therefore, in this study we aimed to: 1) clarify the effectiveness of ASL in lateralizing the seizure onset zone (SOZ) in MTLE by comparing the results from ASL with those from SEEG and its outcome results and 2) assess the correlation between perfusion data from ASL and metabolism data from ^{18}F-FDG PET, which were simultaneously acquired with a PET/MR scanner.

2. Methods

2.1. Patients

Between October 2016 and August 2017, we retrospectively studied 12 patients (mean age: 25 years, range: 17–35 years; male: $N = 6$, female: $N = 6$) who had confirmed pure MTLE diagnosed with semiology, EEG, structural MRI, and SEEG. The patients had a mean seizure duration of 14.00 ± 4.63 years. Table 1 shows the demographics and clinical features of the included patients.

The inclusion criteria were as follows: 1) pure unilateral MTLE, 2) an invasive SEEG evaluation, and 3) ASL and ^{18}F-FDG PET simultaneously acquired with PET/MR. The exclusion criteria were bilateral MTLE or other types of epilepsy and lack of ASL, ^{18}F-FDG PET, or SEEG evaluation.

The 12 patients underwent the same protocol. First, ^{18}F-FDG PET, ASL, and 3D MRI were simultaneously acquired with a PET/MR scanner after long-term video scalp EEG examination. Second, SEEG electrode implantation and electro-clinical evaluation were conducted by a multidisciplinary team (MDT) to precisely localize the SOZ. Subsequently, radiofrequency thermocoagulation (RFTC) was also performed in these patients (unpublished data).

This study was approved by the ethics committee at Xuanwu Hospital and conducted in accordance with the Declaration of Helsinki. All patients provided informed consent prior to their inclusion in the study.

2.2. ^{18}F-FDG PET, ASL, and 3D MRI data acquisition

All patients underwent a static PET scan and the clinical scan protocol was as follows. Each patient was instructed to fast for at least 6 h and had a confirmed serum glucose level below 8 mmol/L; brain images were acquired with the patient in the supine position 60 min after an intravenous injection of 3.7 MBq/kg of 18F-FDG. PET/MR allowed for the simultaneous comparison of PET with ASL under the same conditions. The images were acquired using a GE SIGNA TOF PET/MR system (GE Healthcare, Milwaukee, WI, USA). Simultaneous PET and 3 T MR imaging data were acquired. 3-Tesla MR were conducted with a 19-channel head-neck coil. PET reconstruction was performed with a TOF-OSEM algorithm (time-of-flight ordered subset expectation maximization; 8 iterations and 32 subsets) on a 192 × 192 matrix, 35-cm field-of view, 2.78-mm slice thickness, and included correction for scatter, random counts, dead time, and point spread function (full width at half maximum of a 3.0-mm Gaussian filter). For this integrated PET/MR, attenuation correction was performed with T1WI. The PET acquisition was performed before and after contrast injection. The duration was approximately 10 min for each task.

ASL perfusion imaging was performed simultaneously with the ^{18}F-FDG PET/MR scanning. All ASL scanning independently used the 3D pseudo-continuous arterial spin labeling technique in a region of interest (ROI) and voxel-wise manner. The parameters were as follows: repetition time (TR) = 4809 ms; echo time (TE) = 10.7 ms; post-labeling delay = 2025 ms; field of view (FOV) = 240 × 40 mm; number of excitations (NEX) = 3; spiral readout of 8 arms × 512 samples; 32 × 4.0 mm axial sections with whole brain coverage; and duration = 4 min 39 s.

All patients underwent 3D T1-weighted scans with a sagittal 3D brain volume sequence (FOV = 256 × 256 mm; NEX = 1; TR/TE = 8.5/3.2 ms; flip angle = 15; slice thickness = 1 mm; and duration = 5 min 8 s). Fat saturation was applied.

2.3. SEEG implantation and outcome data

All 12 patients underwent implantation of frameless SEEG electrodes (Alcis, Besancon, France) with the guidance of Robotic Stereotactic Assistance (Medtech, Montpellier, France). The contacts mainly covered the area of the mesial temporal lobe of the ipsilateral side. The others were mainly distributed across the frontal and insular lobes in cases of temporal plus epilepsy. In most patients, there was further implantation in the contralateral hippocampus in cases of bitemporal lobe epilepsy.

After implantation, all patients underwent long-term intracranial SEEG recording until at least one ictal onset EEG was captured. The invasive EEG recordings of both the interictal and ictal periods were analyzed by the MDT. The SOZ was defined from the SEEG recordings using the standard as: 1) low-voltage fast activity over 20 Hz, 2) recruiting fast discharge (around 10 Hz or more) of spikes or polyspikes, and 3) rhythmic activity (around 10 Hz) of low amplitude (David et al., 2011). Brain mapping and electro-stimulation were conducted before RFTC. The outcome was categorized following Engel's classification (Engel Jr., 1993).

2.4. Quantitative hippocampus volume analysis

Given that our patients had pure unilateral MTLE, we chose the ipsilateral hippocampus, which was individually segmented, as the object of our analysis. For individual patients, the 3D-T1 image was processed for cortical reconstruction and volumetric segmentation with the standard FreeSurfer image analysis v5.3.0 package, according to the developer's online guidelines (http://www.freesurfer.net/fswiki/DownloadAndInstall). Bilateral hippocampal volumes were quantitatively assessed, with the bilateral hippocampus extracted as a ROI for further analysis. Furthermore, the T1 image in the right-anterior-

Table 1
Patient characteristics.

Pt	Sex	Age (years)	Seizure duration (years)	Type of seizure	Frequency	Number of AEDs	Etiology/MRI findings	EEG* (side/area)	SEEG	PET	ASL	Follow-up (months)	Engel
1	M	26	19	Complex partial	2–4/month	3	R HS	R/T Fr	R	R	R	9	IA
2	F	17	8	Complex partial/GTCS	1–2/month	3	L HS	L/Hemi	L	L	L	12	IB
3	F	27	12	Complex partial	10/month	4	R HS	B/T	R	R	R	8	II
4	F	35	20	Complex partial	1–2/week	3	R HS	B/T	R	R	R	4	IA
5	F	19	12	Complex partial/GTCS	4–5/month	3	L HS	L/Fr	L	L	L	13	IA
6	M	18	18	Simple partial	2–3/week	3	L HS	N	L	L	L	11	IB
7	M	30	14	Complex partial	2–4/month	4	R HS	N	R	R	R	4	IA
8	F	27	13	Complex partial/GTCS	1–2/month	3	L HS	L/Hemi	L	L	L	13	IB
9	F	28	17	Complex partial	12/month	4	R HS	R/T	R	R	R	4	IA
10	M	27	16	GTCS	6/year	3	R HS	R/T Fr	R	R	R	12	IB
11	M	32	15	Complex partial	2–3/week	4	R HS	R/T	R	R	R	11	II
12	M	19	4	Complex partial	2–3/day	2	L HS	B/T	L	L	L	7	III

Pt: patient; M: male; F: female; GTCS: generalized tonic-clonic seizures; R: right; L: left; B: bilateral; HS: hippocampus sclerosis; Fr: frontal; T: temporal; Hemi: hemisphere; N: normal; EEG: electroencephalography; SEEG: stereoelectroencephalography; ASL: arterial spin labeling; AED: antiepileptic drug.

* All patients underwent a 3–4 h scalp-EEG with no seizure onset, and the EEG-based lateralization and localization information were determined by the area of the epileptic discharges during the interictal phase.

superior coordination space was also obtained.

The hippocampus volume index (HVI) can be calculated with the following formula: HVI = hippocampus volume × 100/total intracranial volume (Granados Sanchez and Orejuela Zapata, 2017). Here, the ipsilateral side was defined as the side of the seizure foci. Thus, the contralateral and ipsilateral HVIs were compared with the Wilcoxon signed-rank test with statistical significance determined as $p < 0.05$.

2.5. ^{18}F-FDG PET, CBF, and 3D MRI data analysis

Image analysis was conducted with tools from the FMRIB Software Library (https://fsl.fmrib.ox.ac.uk/fsl/fslwiki/FslInstallation). The quantitative FDG-PET and CBF data analyses were voxel-based, which may be of additional value compared with the visual qualitative analysis. Non-brain tissue was first removed from the structural MR images with the Brain Extraction Tool. Subsequently, we conducted linear registration with the FMRIB Linear Registration Tool to normalize co-registered CBF maps derived from ASL and PET with structural MRI using 6 degrees of freedom and the mutual information cost function. The spatial resolution of the registered ASL in all directions was smoothed with a 6-mm FWHM after reconstruction with SPM8 (http://www.fil.ion.ucl.ac.uk/spm/software/spm8/). We extracted the bilateral hippocampus as a mask from the ASL and PET images, which provided quantitative information on perfusion and metabolism, respectively. To reduce inter-subject variance before performing statistical analysis, the voxel value for each patient's PET and ASL images was divided by the average voxel value measured in the cerebellum. The reasons were as follows: 1) the cerebellum is unlikely to be hypermetabolic in epilepsy. For the temporal lobes to be considered hypometabolic, these references must indeed be hypometabolic. This renders the finding of cortical hypometabolism relative to total cerebellar cortex metabolism more robust. 2) Cortical reference sites outside the temporal lobes may be involved in patients with extratemporal epilepsy. 3) Brain activity due to thinking or uncontrollable sensory input, particularly visual, or intermittent use of motor areas such as the frontal eye fields may alter (increase) extratemporal cortical metabolic rates (Blum et al., 1998). We compared the normalized average voxel value of perfusion from ASL and metabolism from PET between the contralateral and ipsilateral hippocampus with the Wilcoxon signed rank test ($p < 0.05$).

Next, we calculated the asymmetry index (AI) with the following formula (Lim et al., 2008):

$$AI = (\text{ipsilateral} - \text{contralataral})/[\text{ipsilateral}+\text{contralateral}/2]$$

Therefore, the AI values for the bilateral hippocampus (hippocampus metabolism AI, HMAI; hippocampus perfusion AI, HPAI) can thereby be separately calculated for each patient. To investigate correlations, we calculated Pearson's correlation coefficient between AI values with Matlab R2015a (Mathworks, Natick, Mass, USA). We interpreted the correlations as follows: 0.0–0.2 = slight; 0.2–0.4 = fair; 0.4–0.6 = moderate; 0.6–0.8 = substantial; 0.8–1.0 = almost perfect (Richard Landis and Koch, 1977). Wilcoxon signed rank tests were calculated with the Statistical Package for the Social Sciences for Windows (Version 22; IBM, Armonk, New York, USA).

3. Results

3.1. EEG, SEEG, and outcome

In our 12 patients, we observed a series of abnormal discharges during the interictal phases and rapid changes at ictal onset in the mesial temporal area. We also observed abnormal discharges in most patients ($N = 10$), with some showing bilateral changes in the scalp EEG.

A total of 85 electrodes were implanted (average, 7.09 ± 0.79). Regarding the SEEG recordings, we did not observe any propagation to the lateral temporal area or extra-temporal lobe structures (Fig. 1). All patients had definite lateralization after long-term monitoring (right side, $N = 7$; left side, $N = 5$) without bilateral temporal lobe epilepsy. In our 12 patients, nine (75%) achieved Engel class I with a mean follow-up of 9.00 ± 3.54 months (Table 1).

3.2. Comparison of ^{18}F-FDG PET, ASL, and SEEG

Table 2 presents the mean normalized voxel values of perfusion from ASL and metabolism from PET. In our 12 patients, we observed a mean normalized voxel value of ASL from the contralateral hippocampus of 0.97 ± 0.19 (range: 0.65–1.43) and from the ipsilateral hippocampus of 0.84 ± 0.14 (range: 0.59–1.17). This represents a significant difference between the two hemispheres (Wilcoxon signed rank test, $p < 0.05$), with lower perfusion on the ipsilateral side. As for PET, we observed a mean normalized voxel value in the contralateral hippocampus of 1.07 ± 0.30 (range: 0.80–1.75), while there was a significantly lower mean voxel value on the ipsilateral side using the Wilcoxon signed rank test (0.86 ± 0.20; range: 0.66–1.33; $p < 0.05$).

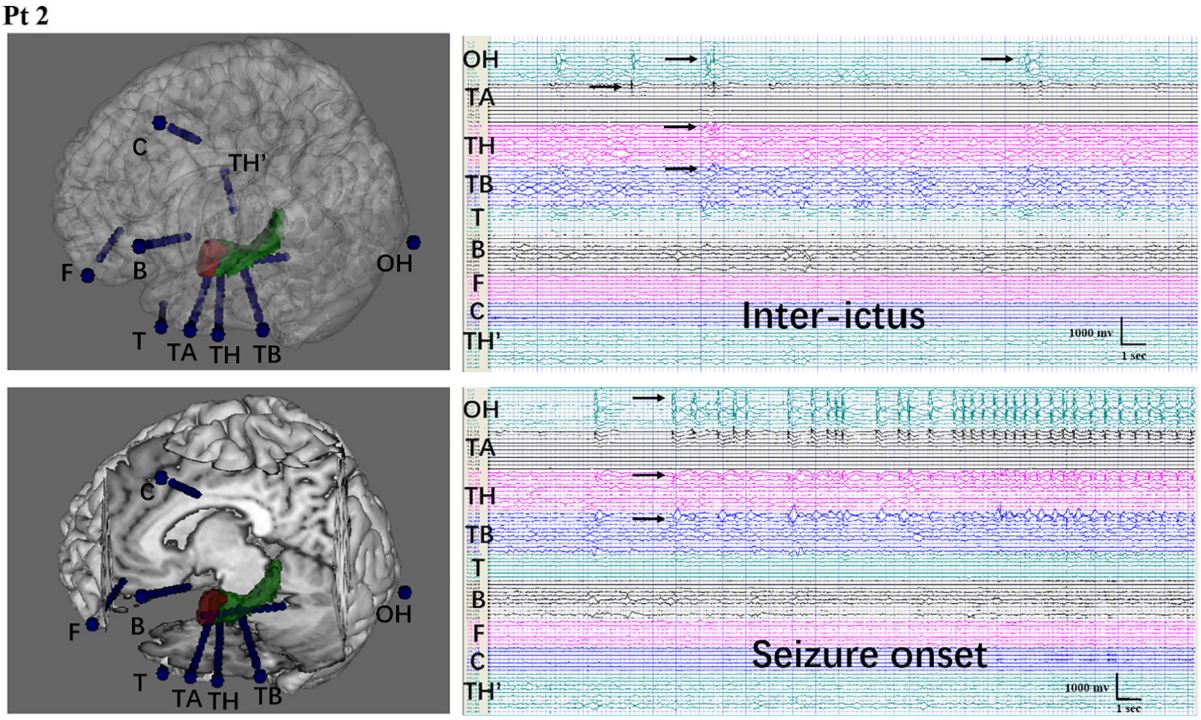

Fig. 1. Reconstruction and stereoelectroencephalography (SEEG) recordings from patient 2 (left mesial temporal lobe epilepsy, MTLE)
A–B: 3D reconstruction of nine electrodes and the spatial relationship between the electrodes and relative brain structure. OH, TH, and TB were implanted in the hippocampus. TA was implanted in the amygdala. TH′ was placed in the contralateral hippocampus.
C: SEEG recordings of the interictal phase. Abnormal discharges can be seen in the left hippocampus and amygdala.
D: SEEG manifestation at seizure onset. Rhythmic high amplitude discharges can be seen in the ipsilateral hippocampus and amygdala. There was no propagation to the lateral temporal area or extra-temporal lobe structures, with no abnormalities in the right hippocampus. The patient was evaluated as Engel IB at the 12-month follow up.

Table 2
Statistical results.

Pt	nPET-L	nPET-R	nASL-L	nASL-R	HVIL	HVIR	HMAI	HPAI
1	0.93	0.74	0.99	0.85	0.31	0.24	−0.23	−0.15
2	0.66	0.80	0.89	0.97	0.20	0.22	−0.19	−0.08
3	0.86	0.71	0.91	0.78	0.34	0.20	−0.19	−0.15
4	1.04	0.85	0.94	0.81	0.35	0.25	−0.20	−0.14
5	1.62	1.19	1.06	0.84	0.22	0.29	−0.31	−0.23
6	0.77	0.93	1.02	1.11	0.22	0.31	−0.18	−0.08
7	1.05	0.88	0.97	0.83	0.34	0.31	−0.18	−0.16
8	0.79	0.98	0.73	0.85	0.19	0.28	−0.21	−0.16
9	0.92	0.77	0.85	0.78	0.32	0.24	−0.18	−0.08
10	1.75	1.33	1.43	1.17	0.53	0.15	−0.27	−0.20
11	0.99	0.78	0.65	0.59	0.29	0.19	−0.24	−0.09
12	0.82	0.91	0.83	0.90	0.22	0.30	−0.11	−0.08

nPET-L: normalized left hippocampus average voxel value of PET; nPET-R: normalized right hippocampus average voxel value; nASL-L: normalized left hippocampus average voxel value of ASL; nASL-R: normalized right hippocampus average voxel value of ASL; HVIL: left hippocampus volume index; HVIR: right hippocampus volume index; HMAI: hippocampus metabolism asymmetry index; HPAI: hippocampus perfusion asymmetry index.

We observed relatively low metabolism and perfusion in the ipsilateral hippocampus in our 12 patients. Single-rater visual interpretation suggested that the area of low metabolism visualized with PET tended to be larger than the area of decreased perfusion visualized with ASL. No inter-rater reliability for these assessments were conducted (Fig. 2). Our results suggest that ASL can be effectively used to lateralize the SOZ in patients with MTLE, with results comparable to those obtained by SEEG recordings.

Table 2 shows the AI values calculated for the two groups, while Fig. 3 presents scatter plots of the AI values in the two groups. There was a significant correlation between the AI values from PET and ASL using Pearson's correlation coefficient ($r = 0.72$, $p < 0.05$; Table 3).

3.3. Hippocampal volume analysis

Table 2 also shows the HVIs for each individual patient. The mean HVI of the contralateral hippocampus was 0.32 ± 0.07 (range: 0.22–0.53) while the HVI of the ipsilateral hippocampus was 0.21 ± 0.04 (range: 0.15–0.31). These values were statistically significantly different (Wilcoxon signed rank test, $p < 0.05$; Table 3). In all 12 patients, we observed lower volumes in the ipsilateral hippocampus, which in some cases could be visually detected with structural imaging. These results are in line with the SEEG findings and clinical localizations. Fig. 4 presents the distribution of the HVI values in our 12 patients.

4. Discussion

In our retrospective study, we demonstrated a strong correlation between metabolism measured with PET and perfusion measured with ASL in MTLE. To our knowledge, this is the only report to have systematically employed the SEEG technique and outcomes to assess the effectiveness of ASL in lateralizing the SOZ in MTLE compared with simultaneous acquisition of ^{18}F-FDG PET.

ASL is a newly developed MRI technique to measure perfusion, which has mostly been used in research, although it is increasingly being applied in clinical practice. Moreover, the development of quantification measures will contribute to increasing the diagnostic accuracy of ASL (Brown et al., 2007). Some reports have previously verified the ability of ASL to localize the seizure focus. Many such studies have qualified the usefulness of ASL by visually comparing it with PET, but lacked quantification (Kim et al., 2016; Matsuura et al.,

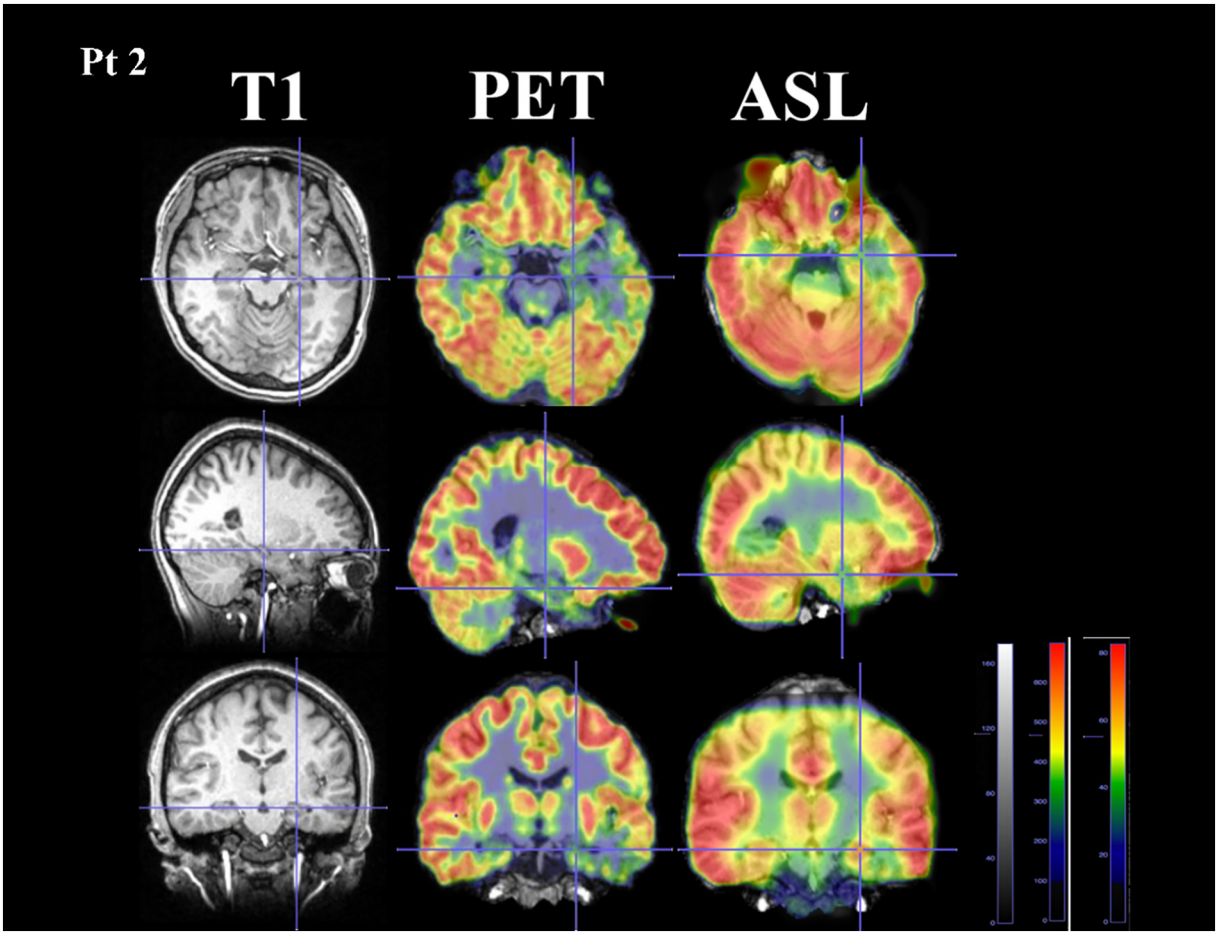

Fig. 2. Comparison between arterial spin labeling (ASL) and positron emission tomography (PET) from patient 2 who was diagnosed with left mesial temporal lobe epilepsy
Hypoperfusion visualized by ASL was consistent with hypometabolism visualized by PET on the left hippocampal area. The area was relatively larger in PET images compared with that in ASL by qualitative assessment.

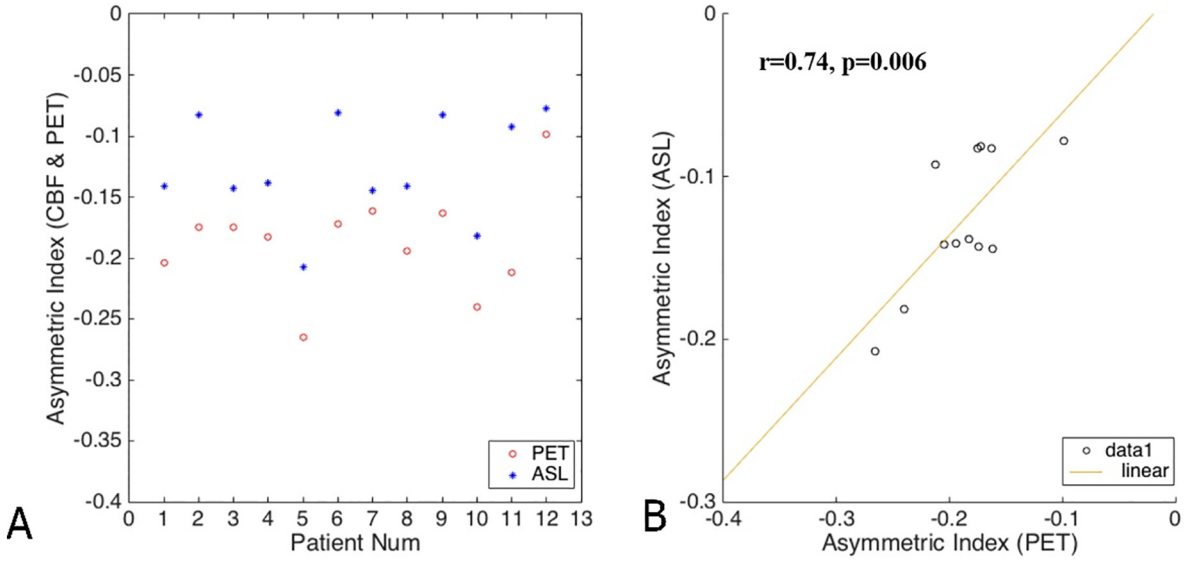

Fig. 3. Scatter plot of asymmetry index values and Pearson's correlations
A: Scatter plot of 12 patients' AI values in PET and ASL. All the AI values in PET and ASL were negative showing that the metabolism and perfusion on the ipsilateral side were relatively decreased.
B: We observed a significant correlation between arterial spin labeling and positron emission tomography (Pearson's correlation, $r = 0.74$, $p = 0.006$).

Table 3
Comparing hippocampal volume indices (HVIs), positron emission tomography (PET) data, and arterial spin labeling (ASL) data between contralateral and ipsilateral sides.

	Z-value	*p*-value	Correlation(r)
Contralateral & ipsilateral HVI	−3.064	0.002*	
Contralateral & ipsilateral PET	−3.059	0.002	
Contralateral & ipsilateral ASL	−3.059	0.002	
HMAI & HPAI		0.006**	0.74

(*) Wilcoxon signed-rank test; (**) Pearson's correlation.

2015).

In our 12 patients, the diagnosis of pure unilateral MTLE was confirmed with structural images, semiology, SEEG recordings, and surgical outcomes. The SEEG technique has been increasingly used as a minimally-invasive way to precisely localize SOZ with the advantage of allowing a three-dimensional definition of the epileptogenic zone (Minotti et al., 2018). In our 12 patients, SEEG was used not only for better localization of SOZ in patients with MTLE, but also for the RFTC approach as a further treatment for epilepsy. We found that seizures were mostly well controlled after RFTC (Engel I: 75% of patients), which was similar to the findings of previous studies (Kramska et al., 2017; Malikova et al., 2014). The invasive EEG results and middle-term surgical outcomes were used as the gold standards to confirm the diagnosis and localization of MTLE. Thus, we restricted our quantitative analysis to a single ROI, the bilateral hippocampus. We calculated the normalized average voxel values to compare perfusion from ASL and metabolism from PET, which can quantify changes in perfusion and metabolism changes in MTLE. Thus, we assessed the effectiveness of ASL to lateralize MTLE, which showed excellent consistency with findings of the invasive assessments. We also observed a significant difference between perfusion in the ipsilateral and contralateral hippocampus, which showed the presence of hypoperfusion in patients with MTLE ($p < 0.05$). The hypoperfusion visualized with ASL is consistent with hypometabolism visualized with ^{18}FDG PET, suggesting consistency between the cerebral blood flow and functional changes in the mesial temporal lobe during the interictal phase.

The use of ^{18}F-FDG PET to identify areas of hypometabolism during the interictal phase has proven to be an effective and sensitive tool to detect epilepsy foci in presurgical evaluations (Rathore et al., 2014). Some recent studies have compared ASL, PET, and other imaging modalities (Shimogawa et al., 2017; Sierra-Marcos et al., 2016), some of which have quantified their results (Storti et al., 2014). These results showed a good consistency between separately acquired ^{18}F-FDG PET and ASL in detecting epilepsy foci. A major disadvantage of the combined PET/MR systems is the complication with MR-based attenuation correction (Attenberger et al., 2015; Beyer et al., 2008). Moreover, it may require more time and impose more limitations for patients compared with PET/CT (for example, patients with magnetic implants cannot be examined with PET/MR). However, comparisons between the separate acquisitions may inappropriate due to differences in conditions and time. Thus, a better comparison of different modalities under the same conditions can be achieved with the PET/MR system, which ensures that both the PET and ASL procedures will take place simultaneously. Moreover, switching from PET/CT to PET/MR will reduce the radiation exposure caused by the CT aspect of the examination (Hirsch et al., 2013). Therefore, as it was available, the PET/MR was chosen for scanning in this study series, which in a way can be considered as a proof of principle for previous studies using separate systems.

Studies comparing PET and ASL acquired simultaneously with a hybrid PET/MR scanner are rare (Boscolo Galazzo et al., 2016). Boscolo Galazzo et al. (2016) assumed that simultaneous functional acquisition of PET and ASL can allow more accurate comparisons and better results, as the acquisitions occur under the same physiological or pathophysiological conditions. They assessed concordance between ASL and PET similarly using AI values, and observed high agreement between the two ($r_s = 0.49$, $p < 0.0005$), which is consistent with the results of the present study. However, their study lacked the use of invasive SEEG evaluation and treatment outcome as gold standards, as we have used here. We compared metabolism and perfusion in the hippocampus of patients with MTLE and observed a significant correlation between the two parameters ($r = 0.74$, $p = 0.006$), which was opposite to the findings of a previous study (Lim et al., 2008). Compared with PET, ASL has several benefits in that it avoids exposing patients to radioactive substances and involves lower cost and greater time-efficiency (Wolf and Detre, 2007). In addition, previous studies have used 1.5T MRI for ASL scanning for detecting the epileptogenic zone (Blauwblomme et al., 2014; Kim et al., 2016), which certified its reliability with 1.5 T MRI.

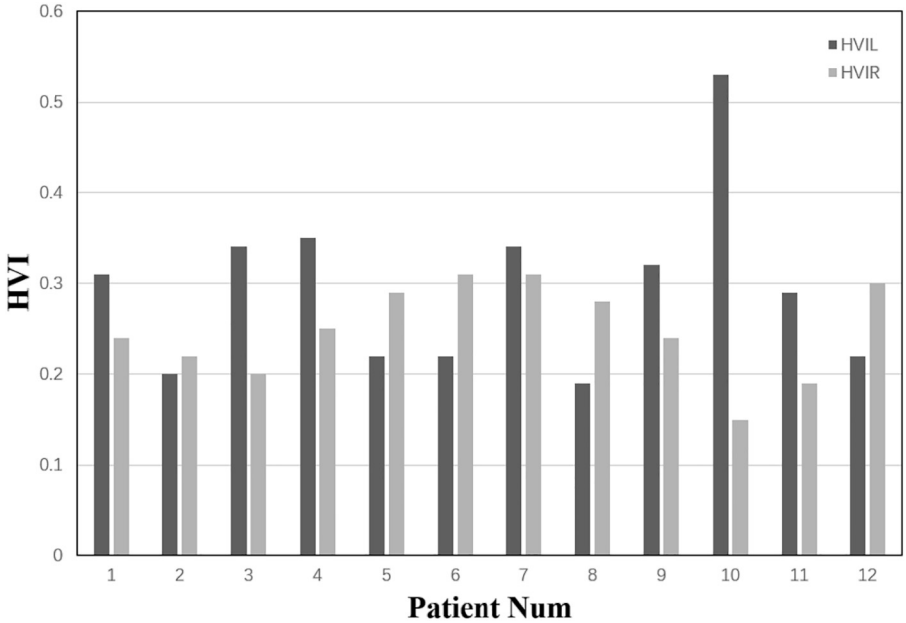

Fig. 4. Distribution of the hippocampal volume indices in the 12 patients
We observed decreased volume of the left hippocampus in patients 2, 5, 6, 8, and 12, with the other patients showing hippocampal atrophy on the right side.

This completely non-invasive diagnostic method offers an alternative choice for presurgical evaluation, especially when PET/CT or PET/MR is not available at a medical center or their use is limited to specific situations.

We also quantitatively measured the volume of the hippocampus and observed that the ipsilateral hippocampus was significantly smaller than the contralateral side ($p < 0.05$). Atrophy of the hippocampus may offer further diagnostic evidence of MTLE, which provides quantified indications of structural changes of the mesial temporal lobe.

Our study is subject to some limitations. A small sample size was obtained, and a larger sample is required to further evaluate the complementary role of ASL compared with PET. Furthermore, other types of epilepsy (e.g., frontal and insular lobe epilepsy) should also be investigated to assess the effectiveness of ASL in detecting the SOZ. Additionally, dynamic FDG-PET analysis may be needed for further investigation. Finally, other regions of the mesial temporal lobe will be assessed in our future investigations; the hippocampus was the only ROI in this study for both ASL and PET. Our results can only prove that ASL can help in the lateralization of MTLE.

5. Conclusion

In conclusion, ASL appears to be a reliable and complementary tool for MTLE lateralization compared to the simultaneously acquired PET with a PET/MR scanner. This non-invasive modality may offer an attractive alternative when PET/CT or PET/MR is not available at a medical center or their use is limited to specific situations.

Acknowledgements

The authors want to thank Minjing Hu from the Department of Neurology, Affiliated Hospital to Nantong University for offering technical assistance.

None of the authors have conflicts of interest relevant to this article.

This work was funded by the Key Project with Capital Characteristics (Beijing Municipal Science and Technology Commission, Z161100000516008).

References

Attenberger, U., Catana, C., Chandarana, H., Catalano, O.A., Friedman, K., Schonberg, S.A., Thrall, J., Salvatore, M., Rosen, B.R., Guimaraes, A.R., 2015. Whole-body FDG PET-MR oncologic imaging: pitfalls in clinical interpretation related to inaccurate MR-based attenuation correction. Abdom. Imaging 40, 1374–1386.

Beyer, T., Weigert, M., Quick, H.H., Pietrzyk, U., Vogt, F., Palm, C., Antoch, G., Muller, S.P., Bockisch, A., 2008. MR-based attenuation correction for torso-PET/MR imaging: pitfalls in mapping MR to CT data. Eur. J. Nucl. Med. Mol. Imaging 35, 1142–1146.

Blauwblomme, T., Boddaert, N., Chemaly, N., Chiron, C., Pages, M., Varlet, P., Bourgeois, M., Bahi-Buisson, N., Kaminska, A., Grevent, D., Brunelle, F., Sainte-Rose, C., Archambaud, F., Nabbout, R., 2014. Arterial spin labeling MRI: a step forward in non-invasive delineation of focal cortical dysplasia in children. Epilepsy Res. 108, 1932–1939.

Blum, D.E., Ehsan, T., Dungan, D., Karis, J.P., Fisher, R.S., 1998. Bilateral temporal hypometabolism in epilepsy. Epilepsia 39, 651–659.

Boscolo Galazzo, I., Storti, S.F., Del Felice, A., Pizzini, F.B., Arcaro, C., Formaggio, E., Mai, R., Chappell, M., Beltramello, A., Manganotti, P., 2015. Patient-specific detection of cerebral blood flow alterations as assessed by arterial spin labeling in drug-resistant epileptic patients. PLoS One 10, e0123975.

Boscolo Galazzo, I., Mattoli, M.V., Pizzini, F.B., De Vita, E., Barnes, A., Duncan, J.S., Jager, H.R., Golay, X., Bomanji, J.B., Koepp, M., Groves, A.M., Fraioli, F., 2016. Cerebral metabolism and perfusion in MR-negative individuals with refractory focal epilepsy assessed by simultaneous acquisition of (18)F-FDG PET and arterial spin labeling. Neuroimage Clin. 11, 648–657.

Brown, G.G., Clark, C., Liu, T.T., 2007. Measurement of cerebral perfusion with arterial spin labeling: part 2. Applications. J. Int. Neuropsychol. Soc. 13, 526–538.

Chavakula, V., Cosgrove, G.R., 2017. Imaging for epilepsy surgery. Semin. Neurol. 37, 580–588.

David, O., Blauwblomme, T., Job, A.S., Chabardes, S., Hoffmann, D., Minotti, L., Kahane, P., 2011. Imaging the seizure onset zone with stereo-electroencephalography. Brain 134, 2898–2911.

Detre, J.A., Leigh, J.S., Williams, D.S., Koretsky, A.P., 1992. Perfusion imaging. Magn. Reson. Med. 23, 37–45.

Ding, Y.S., Chen, B.B., Glielmi, C., Friedman, K., Devinsky, O., 2014. A pilot study in epilepsy patients using simultaneous PET/MR. Am. J. Nucl. Med. Mol. Imaging 4, 459–470.

Duncan, J.S., 2010. Imaging in the surgical treatment of epilepsy. Nat. Rev. Neurol. 6, 537–550.

Engel Jr., J., 1993. Update on surgical treatment of the epilepsies. Summary of the second international palm desert conference on the surgical treatment of the epilepsies (1992). Neurology 43, 1612–1617.

Fisher, R.S., Stein, A., Karis, J., 1997. Epilepsy for the neuroradiologist. AJNR Am. J. Neuroradiol. 18, 851–863.

Fraioli, F., Punwani, S., 2014. Clinical and research applications of simultaneous positron emission tomography and MRI. Br. J. Radiol. 87, 20130464.

Granados Sanchez, A.M., Orejuela Zapata, J.F., 2017. Diagnosis of mesial temporal sclerosis: sensitivity, specificity and predictive values of the quantitative analysis of magnetic resonance imaging. Neuroradiol. J. 31, 50–59 (1971400917731301).

Hardy, S.G., Miller, J.W., Holmes, M.D., Born, D.E., Ojemann, G.A., Dodrill, C.B., Hallam, D.K., 2003. Factors predicting outcome of surgery for intractable epilepsy with pathologically verified mesial temporal sclerosis. Epilepsia 44, 565–568.

Hirsch, F.W., Sattler, B., Sorge, I., Kurch, L., Viehweger, A., Ritter, L., Werner, P., Jochimsen, T., Barthel, H., Bierbach, U., Till, H., Sabri, O., Kluge, R., 2013. PET/MR in children. Initial clinical experience in paediatric oncology using an integrated PET/MR scanner. Pediatr. Radiol. 43, 860–875.

Kim, B.S., Lee, S.T., Yun, T.J., Lee, S.K., Paeng, J.C., Jun, J., Kang, K.M., Choi, S.H., Kim, J.H., Sohn, C.H., 2016. Capability of arterial spin labeling MR imaging in localizing seizure focus in clinical seizure activity. Eur. J. Radiol. 85, 1295–1303.

Kramska, L., Vojtech, Z., Lukavsky, J., Stara, M., Malikova, H., 2017. Five-year neuropsychological outcome after stereotactic radiofrequency amygdalohippocampectomy for mesial temporal lobe epilepsy: longitudinal study. Stereotact. Funct. Neurosurg. 95, 149–157.

Lim, Y.M., Cho, Y.W., Shamim, S., Solomon, J., Birn, R., Luh, W.M., Gaillard, W.D., Ritzl, E.K., Theodore, W.H., 2008. Usefulness of pulsed arterial spin labeling MR imaging in mesial temporal lobe epilepsy. Epilepsy Res. 82, 183–189.

Malikova, H., Kramska, L., Vojtech, Z., Liscak, R., Sroubek, J., Lukavsky, J., Druga, R., 2014. Different surgical approaches for mesial temporal epilepsy: resection extent, seizure, and neuropsychological outcomes. Stereotact. Funct. Neurosurg. 92, 372–380.

Matsuura, K., Maeda, M., Okamoto, K., Araki, T., Miura, Y., Hamada, K., Kanamaru, K., Tomimoto, H., 2015. Usefulness of arterial spin-labeling images in periictal state diagnosis of epilepsy. J. Neurol. Sci. 359, 424–429.

Minotti, L., Montavont, A., Scholly, J., Tyvaert, L., Taussig, D., 2018. Indications and limits of stereoelectroencephalography (SEEG). Neurophysiol Clin. 48, 15–24.

Rakheja, R., Demello, L., Chandarana, H., Glielmi, C., Geppert, C., Faul, D., Friedman, K.P., 2013. Comparison of the accuracy of PET/CT and PET/MRI spatial registration of multiple metastatic lesions. AJR Am. J. Roentgenol. 201, 1120–1123.

Rathore, C., Dickson, J.C., Teotonio, R., Ell, P., Duncan, J.S., 2014. The utility of 18F-fluorodeoxyglucose PET (FDG PET) in epilepsy surgery. Epilepsy Res. 108, 1306–1314.

Richard Landis, J., Koch, G.G., 1977. Themeasurement of observer agreement for categorical data. Biometrics 33, 159–174.

Rosenow, F., Luders, H., 2001. Presurgical evaluation of epilepsy. Brain 124, 1683–1700.

Shimogawa, T., Morioka, T., Sayama, T., Haga, S., Kanazawa, Y., Murao, K., Arakawa, S., Sakata, A., Iihara, K., 2017. The initial use of arterial spin labeling perfusion and diffusion-weighted magnetic resonance images in the diagnosis of nonconvulsive partial status epileptics. Epilepsy Res. 129, 162–173.

Sierra-Marcos, A., Carreno, M., Setoain, X., Lopez-Rueda, A., Aparicio, J., Donaire, A., Bargallo, N., 2016. Accuracy of arterial spin labeling magnetic resonance imaging (MRI) perfusion in detecting the epileptogenic zone in patients with drug-resistant neocortical epilepsy: comparison with electrophysiological data, structural MRI, SISCOM and FDG-PET. Eur. J. Neurol. 23, 160–167.

Storti, S.F., Boscolo Galazzo, I., Del Felice, A., Pizzini, F.B., Arcaro, C., Formaggio, E., Mai, R., Manganotti, P., 2014. Combining ESI, ASL and PET for quantitative assessment of drug-resistant focal epilepsy. Neuroimage 102 (Pt 1), 49–59.

Tudisca, C., Nasoodi, A., Fraioli, F., 2015. PET-MRI: clinical application of the new hybrid technology. Nucl. Med. Commun. 36, 666–678.

Williams, D.S., Detre, J.A., Leigh, J.S., Koretsky, A.P., 1992. Magnetic resonance imaging of perfusion using spin invesion of arterial water. Proc. Natl. Acad. Sci. U. S. A. 89, 212–216.

Wolf, R.L., Detre, J.A., 2007. Clinical neuroimaging using arterial spin-labeled perfusion magnetic resonance imaging. Neurotherapeutics 4, 346–359.

Wolf, R.L., Alsop, D.C., Levy-Reis, I., Meyer, P.T., Maldjian, J.A., Gonzalez-Atavales, J., French, J.A., Alavi, A., Detre, J.A., 2001. Detection of mesial temporal lobe hypoperfusion in patients with temporal lobe epilepsy by use of arterial spin labeled perfusion MR imaging. AJNR Am. J. Neuroradiol. 22, 1334–1341.